



Novel sizing role of 3D transesophageal echocardiography in a novel left atrial appendage clip device for patients undergoing video-assisted atrial fibrillation ablation: a cohort study

Fujian Duan^{1#}, Hui Li^{1#}, Chenghui Zhou², Haojie Li³, Jia Tao¹, Wenying Kang², Minggang Yu³, Zhe Zheng³

¹Department of Echocardiography, State Key Laboratory of Cardiovascular Disease, Fuwai Hospital, National Center for Cardiovascular Diseases, Chinese Academy of Medical Sciences and Peking Union Medical College, Beijing, China; ²Department of Anesthesiology, State Key Laboratory of Cardiovascular Disease, Fuwai Hospital, National Center for Cardiovascular Diseases, Chinese Academy of Medical Sciences and Peking Union Medical College, Beijing, China; ³Department of Cardiovascular Surgery, State Key Laboratory of Cardiovascular Disease, Fuwai Hospital, National Center for Cardiovascular Diseases, Chinese Academy of Medical Sciences and Peking Union Medical College, Beijing, China

Contributions: (I) Conception and design: F Duan, Hui Li, Z Zheng; (II) Administrative support: Z Zheng; (III) Provision of study materials or patients: F Duan, Hui Li, Haojie Li, Z Zheng; (IV) Collection and assembly of data: F Duan, Hui Li, C Zhou, Haojie Li, J Tao, W Kang, M Yu; (V) Data analysis and interpretation: F Duan, Hui Li; (VI) Manuscript writing: All authors; (VII) Final approval of manuscript: All authors.

[#]These authors contributed equally to this work.

Correspondence to: Zhe Zheng, MD. Department of Cardiovascular Surgery, State Key Laboratory of Cardiovascular Disease, Fuwai Hospital, National Center for Cardiovascular Diseases, Chinese Academy of Medical Sciences and Peking Union Medical College, 167 Beilishi Road, Beijing 100037, China. Email: zhengzhe@fuwai.com.

Background: Three-dimensional (3D) transesophageal echocardiography (TEE) has been successfully used in the sizing of left atrial appendage (LAA) occlusion devices, but its use has not yet been studied in LAA clip devices. We sought to develop and validate the novel use of 3D-TEE sizing in a novel LAA clip device for atrial fibrillation (AF) patients undergoing video-assisted thoracic surgery (VATS) ablation.

Methods: Consecutive patients with isolated AF undergoing LAA clipping or excision during VATS ablation were included in the study between June 2021 and September 2022 at Fuwai Hospital. The patients underwent 3D-TEE examinations preoperatively and postoperatively. The VATS length, LAA clip effective length, and LAA excision margin length were recorded. A correlation analysis, intraclass correlation coefficient (ICC) analysis, and Bland-Altman plot analysis were conducted to examine the TEE parameters, VATS length, LAA clip effective length, and LAA excision margin length.

Results: In total, 26 AF patients undergoing LAA clipping and 15 undergoing LAA excision were included in the study. In the LAA clipping group, in which the Atriclip size served as the control, the 3D-TEE with volumetric measurement (the perimeter-derived maximum orifice diameter) ($R=0.938$; $ICC=0.934$; Bland-Altman plot variability, 3.85%) showed the best sizing efficacy for the LAA clip device among the 3D-TEE with multiplanar reformatting sizing (the perimeter-derived maximum orifice diameter) ($R=0.808$; $ICC=0.772$; Bland-Altman plot variability, 3.85%), VATS sizing ($R=0.851$; $ICC=0.756$; Bland-Altman plot variability, 11.54%), and VATS plus 0.5-cm sizing ($R=0.851$; $ICC=0.775$; Bland-Altman plot variability, 11.54%) measurements (all $P<0.001$). In addition, for the distribution of matched sizing in the LAA clip group, 3D-TEE with volumetric measurement sizing (20/26) had a higher proportion than 3D-TEE with multiplanar reformatting sizing (11/26, $P=0.011$), VATS sizing (9/26, $P=0.002$), and VATS plus 0.5-cm sizing (14/26, $P=0.08$). Using the LAA excision margin length as the control, the mean difference in the LAA diameter was 1.17 cm [95% confidence interval (CI): 0.71–1.62 cm, $P<0.001$] in the maximum orifice diameter of two-dimensional-TEE, 0.15 cm (95% CI: -0.32 to 0.61 cm, $P=0.523$) in the perimeter-derived

3D multiplanar reformatting (the maximum orifice diameter), and 0.03 cm (95% CI: -0.47 to 0.53, $P=0.901$) in the perimeter-derived 3D volumetric (3DV) measurement (the maximum orifice diameter), and the related Pearson correlation coefficients for these modalities were 0.760 ($P=0.001$), 0.843 ($P<0.001$), and 0.963 ($P<0.001$), respectively.

Conclusions: Our study showed that 3D-TEE might be employed in the sizing of a novel LAA clip device using the VATS approach in patients with AF. The 3DV measurement (the perimeter-derived maximum orifice diameter) was superior to the VATS measurement. These findings might also apply to LAA VATS excision patients with AF.

Keywords: Three-dimensional transesophageal echocardiography (3D-TEE); left atrial appendage (LAA); Atrial clip; sizing

Submitted Jun 20, 2023. Accepted for publication Nov 24, 2023. Published online Jan 18, 2024.

doi: 10.21037/qims-23-900

View this article at: <https://dx.doi.org/10.21037/qims-23-900>

Introduction

Atrial fibrillation (AF) is a common cardiac arrhythmia with an approximate incidence of 1–2% in the overall population (1). This arrhythmia has been associated with a five-fold increase in the risk of stroke (2), and thus an increase in the risk of mortality (3). There is accumulating evidence that most of the thrombi (>90%) that result in embolic stroke arise in the left atrial appendage (LAA) in patients with non-valvular AF. Anticoagulation and/or antiplatelet therapy has been used to prevent thrombi formation in the LAA but carries a high risk of bleeding (4–6). Other interventional procedures include traditional surgical or percutaneous techniques of LAA excision. In addition, successful LAA occlusion in open-heart surgery using an epicardial clipping device has also been introduced (7,8). However, the limitations of these methods include radiation and intracardiac operation injuries, such as atrial septal ostomy, and median sternotomy with cardiopulmonary bypass.

In addition to the intracardiac or open-heart approach (9) for the LAA intervention, video-assisted thoracic surgery (VATS) has emerged as a widely used surgical procedure with minimally invasive features for patients with AF (8,10–12). Recently, we designed a novel type of LAA clip device, and successfully introduced its use in AF patients during VATS. Initially, we directly used a thoracoscopic instrument to measure the base of the LAA to size the clip device. However, we have also used intraoperative two-dimensional (2D)—or three-dimensional (3D)—transesophageal echocardiography (TEE) for the LAA assessment after general anesthesia. TEE has been used

as a golden standard method in LAA intracardiac closure (13–18). However, the sizing role of TEE in the novel LAA clip device remains unknown. Thus, we retrospectively analyzed the TEE parameters of the LAA to explore their potential value in this novel LAA clip device sizing, and we verified this non-invasive sizing method in prospectively selected AF patients undergoing LAA excision via VATS. We present this article in accordance with the STROBE reporting checklist (available at <https://qims.amegroups.com/article/view/10.21037/qims-23-900/rc>).

Methods

Study subjects

Consecutive patients with isolated AF undergoing thoracoscopic epicardial ablation between June 2021 and September 2022 at Fuwai Hospital were included in the study. To be eligible for inclusion in this study, the patients had to meet the following inclusion criteria: (I) have symptomatic paroxysmal, persistent, or long-standing persistent AF without concomitant cardiac structural disease; and (II) not be refractory or intolerant to one or more antiarrhythmic drugs. Patients were excluded from the study if they met any of the following exclusion criteria: (I) had a significant structural heart disease; (II) had undergone heart or lung surgery previously; and/or (III) had severe respiratory dysfunction (*Figure 1*). This study was conducted in accordance with the Declaration of Helsinki (as revised in 2013). The study was approved by the Independent Ethics Committee of Fuwai Hospital, and all patients provided written informed consent.

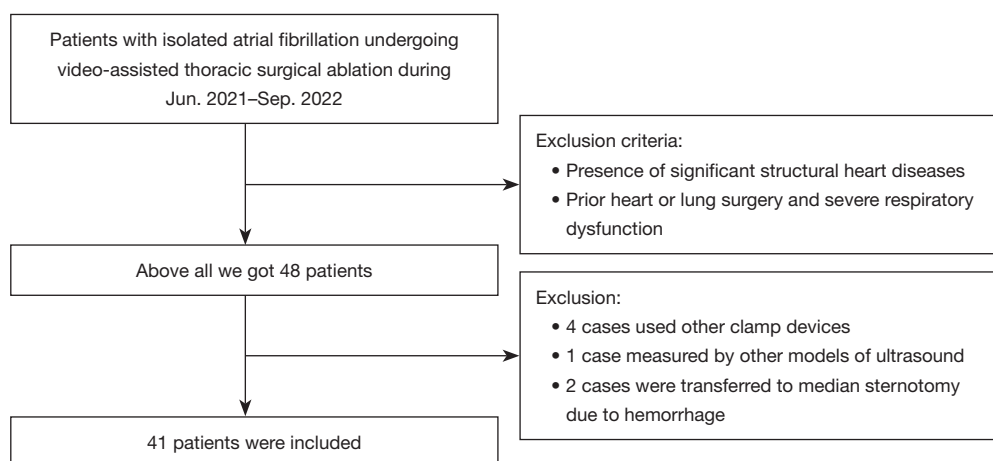


Figure 1 Flow diagram showing the enrollment process for patients.

Anesthesia and TEE

All the patients received standardized general anesthesia and left-sided double lumen endobronchial tube intubation. The effects of lung separation were confirmed by flexible fiberoptic bronchoscopy. All patients received an arterial line and underwent central venous pressure monitoring. Patients' body temperatures were kept at 36.0–36.5 °C via a body surface warming system.

All the patients underwent TEE before and after ablation. Echocardiographic data were recorded using a Philips CVx scanner equipped with an X8-2t 3D (7–15 MHz) probe; Qlab.10.5 (Philips Medical Systems, Andover, MA, USA) analysis software was used for the 3D imaging analysis and 3D data measurement.

Surgical procedure

The ablation surgery was performed using the bilateral thoracic approach without cardiopulmonary bypass support. Generally, a 10-mm, 30° scope was placed through the third intercostal space across the left anterior axillary line. Next, a 15-mm working port was inserted in the fourth intercostal space midaxillary line, and a 10-mm working port was inserted in the second intercostal space midclavicular line. The right-access port was positioned further forward than the left-access port. Left-sided Box lesion ablation was performed with linear lesions, including bilateral pulmonary vein isolation, the roof line, the inferior line, left fibrous trigone lesion, and linear lesion connecting the left upper pulmonary vein to the LAA. Right-sided lesion ablation was also performed, including superior

vena cava-inferior vena cava (SVC-IVC) line, linear lesion connecting the right atrial appendage (RAA) to the SVC-IVC line, and linear lesion connecting the tip to the base of the RAA on the inner wall of the RAA (10). Further, hybrid ablation combining thoracoscopic epicardial ablation with electrophysiological mapping and catheter ablation was introduced to improve the results of VATS for patients with long-standing persistent AF and marked atrial dilation.

The LAA was separated clearly, and then clipped (LAA BARRETTE® SYSTEM, Beijing Comredy Medical Scientific Co., Ltd., Beijing, China) or excised [using a stapling device (EZ60, Ethicon Endosurgery Inc., Cincinnati, USA)] accordingly. The VATS length, Atriclip effective lengths, and LAA excision margin lengths were recorded.

LAA assessment by TEE

Optimal 2D and 3D-TEE images for at least five cardiac cycles were obtained. To simulate the epicardial thoracoscopic procedure of the LAA, we chose the left circumflex artery (LCX) and left superior pulmonary vein (LSPV) orifice (the root of the Coumadin ridge) as the two reference points. In the 2D imaging analysis, we measured the maximum LAA orifice diameter at 0°, 45°, 90°, and 135° views at the left ventricular end-systole. The X-plane method under the 2D-TEE mode was also performed to assess the existence of and differentiate between thrombi and spontaneous echo contrast. In the 3D imaging analysis, both 3D multiplanar reformatting (3DP) and 3D volumetric (3DV) measurement (iCrop method) were performed using

the 3D-Zoom data set with the largest LAA orifice (e.g., the long diameter, short diameter, and perimeter diameter). The 3D y-axis plane went through the longitudinal section of the LAA and LSPV orifice, and the 3D x-axis plane went through the two reference points (the LCX and LSPV orifice) to clearly display the LAA orifice area and boundary line in the 3D z-axis or volumetric view. The 3D-TEE zoom data set of the entire LAA with the clear LSPV orifice in each patient was acquired, stored, and analyzed online using Philips Healthcare Q lab software. The LAA function was expressed using the maximal emptying flow velocity (the average value of the five cardiac cycles) at the middle of the LAA (LAAEV) by the pulse wave Doppler. Simultaneous electrocardiogram monitoring was used to define the end-systole (the start of the QRS wave) of the LAA.

Reproducibility

We randomly selected 15% of all of the participants to assess the intraobserver and interobserver variabilities. Intraobserver variability was evaluated by repeating the measurements on two different occasions. Interobserver variability was evaluated by a second examiner independently performing new measurements.

Statistical analysis

The continuous variables with a normal distribution are presented as the mean \pm standard deviation, and were compared using the Student's *t*-test. The categorical variables were tested by the Chi-squared test or Fisher's exact test ($n < 5$). Both the Bland-Altman method and intraclass correlation coefficient (ICC) test with an agreement analysis were performed to compare the 3DP and 3DV obtained perimeter diameter of the LAA and the effective length of the clip device or excised margin. A repeatability analysis for interobserver and intraobserver agreement was also performed using the ICC test. In relation to the ICC outcomes, values of < 0.5 , 0.5 to < 0.75 , 0.75 to < 0.90 , and ≥ 0.90 indicated poor, moderate, good, and perfect agreement, respectively (19). A two-sided *P* value < 0.05 was considered statistically significant. All the statistical analyses were performed with SPSS 25.0 for Windows (SPSS Inc., Chicago, IL, USA), and Stata software (version 17.0; Stata Corporation, College Station, TX, USA).

Results

Patient characteristics

The clinical baseline characteristics of the 41 patients are shown in *Table 1*. No differences were observed in the baseline characteristics between the LAA clip group and the excision group, except in terms of the proportion of males (84.6% vs. 60.0%, respectively, $P = 0.03$). Overall, the patients had a mean age of 59.3 ± 9.0 years, and a mean body mass index of 27.2 ± 2.9 kg/m². Additionally, 31 (75.6%) patients were males and 10 (24.4%) had a history of stroke. The mean left atrium size was 46.4 ± 6.2 mm, and the mean left ventricular ejection fraction (%) was $63.2\% \pm 7.5\%$. Of the patients, 2 (4.9%) had moderate to severe mitral regurgitation, and 4 (9.8%) had moderate to severe tricuspid regurgitation. Additionally, 34 patients (82.9%) underwent concurrent thoracoscope-assisted radiofrequency ablation, and 23 patients (56.1%) underwent hybrid radiofrequency ablation with cardiologists. The mean surgical duration was 337.5 ± 92.5 minutes. The morphologies of the LAA were categorized as follows: chicken wing ($n = 11$, 26.8%), windsock ($n = 16$, 39.0%), cactus ($n = 11$, 26.8%), and cauliflower ($n = 3$, 7.3%). No thrombosis was detected in the LAA in any of the patients.

Comparison between 2D-TEE, 3D-TEE, VATS, and Atriclip effective length

Using the Atriclip effective length as the control, the mean difference in the LAA long orifice diameter was 1.44 cm [95% confidence interval (CI): 1.08–1.81] in 2D-TEE, 1.69 cm (95% CI: 1.37–2.01) in the 3DP measurement, and 1.50 cm (95% CI: 1.17–1.82) in the 3DV measurement (all $P < 0.001$), and the related Pearson correlation coefficients for these modalities were 0.349 ($P = 0.08$), 0.756 ($P < 0.001$), and 0.898 ($P < 0.001$), respectively. However, all these ICCs showed poor agreement (0.103, 95% CI: -0.073 to 0.363 , $P = 0.037$; 0.133, 95% CI: -0.03 to 0.453 , $P < 0.001$; 0.194, 95% CI: -0.021 to 0.568 , $P < 0.001$; respectively) (*Table 2*).

Using the Atriclip effective length as the control, the mean difference in the LAA orifice diameter was 0.63 cm (95% CI: 0.26–0.99, $P = 0.01$) in the perimeter-derived 3DP measurement (the maximum orifice diameter), 0.40 cm (95% CI: 0.04–0.76, $P = 0.031$) in the perimeter-derived 3DV measurement (the maximum orifice diameter), and 0.33 cm (95% CI: -0.02 to 0.68 , $P = 0.067$) in VATS;

Table 1 Demographic and baseline characteristics

Characteristics	Overall (n=41)	LAA clip (n=26)	LAA excision (n=15)	P value
Age (years)	59.3±9.0	57.8±9.3	61.5±8.3	0.22
Male	31 (75.6)	22 (84.6)	9 (60.0)	0.03
Height (cm)	170.8±8.1	171.5±8.3	169.5±8.1	0.46
Body weight (kg)	79.6±10.4	79.6±11.6	79.7±8.6	0.98
BMI (kg/m ²)	27.2±2.9	27.0±3.4	27.7±2.1	0.47
<24.0	4 (9.8)	4 (15.4)	0	0.20
24.0–27.0	14 (34.1)	7 (26.9)	7 (46.7)	
>27.0	23 (56.1)	15 (57.7)	8 (53.3)	
Clinical history (%)				
Atrial fibrillation				0.47
Persist	85.4	88.5	80.0	
Paroxysmal	14.6	11.5	20.0	
Radiofrequency	53.7	50.0	60.0	0.55
Hypertension	56.1	61.5	46.7	0.25
Hyperlipidemia	26.8	34.6	13.3	0.15
Diabetes mellitus	17.1	19.2	13.3	0.64
Coronary artery disease	14.6	11.5	20.0	0.47
Stroke	24.4	26.9	20.0	0.63
COPD	0.0	0.0	0.0	–
NYHA classification (%)				0.88
1	31.7	30.8	33.3	
2	68.3	69.2	66.7	
Transthoracic echocardiographic parameters				
Left atrial size (mm)	46.4±6.2	45.6±5.8	47.8±6.9	0.22
Left ventricular ejection fraction (%)	63.2±7.5	63.3±6.7	62.9±8.9	0.97
Mitral regurgitation (moderate +) (%)	4.9	0.0	13.3	0.06
Tricuspid regurgitation (moderate +) (%)	9.8	3.8	20.0	0.09
Surgical parameters				
Hybrid procedure (%)	56.1	50.0	66.7	0.30
Concurrent radiofrequency (%)	82.9	88.5	73.3	0.22
PEV (cm/s)	18.6±5.2	18.9±5.7	18.0±4.1	0.62
LAA morphology (%)				0.62
Chicken wing	26.8	30.8	20.0	
Winsock	39.0	42.3	33.3	
Cactus	26.8	23.1	33.3	
Cauliflower	7.3	3.8	13.3	

Table 1 (continued)

Table 1 (continued)

Characteristics	Overall (n=41)	LAA clip (n=26)	LAA excision (n=15)	P value
LAA length-VATS (cm)	3.8±0.6	3.8±0.6	–	–
LAA width-VATS (cm)	3.8±1.1	3.8±1.1	–	–
LAA thickness VATS (cm)	1.0±0.2	1.0±0.2	–	–
Thrombus formation (%)	0.0	0.0	0.0	–
Surgical duration (min)	337.5±92.5	338.1±92.7	339.8±97.8	0.96

Data are expressed as the mean ± standard deviation, or number (percentage) of patients. LAA, left atrial appendage; BMI, body mass index; COPD, chronic obstructive pulmonary disease; NYHA, New York Heart Association; PEV, peak ejection velocity; VATS, video-assisted thoracic surgery.

Table 2 Comparison between 2D-TEE, 3D-TEE, VATS, and Atriclip effective length

Variables	Other measurements (cm)	Atriclip effective length (cm)	P	Mean difference (95% CI)	Pearson correlation		ICC		
					R	P	R (95% CI)	P	
2D-TEE vs.									
Long orifice diameter	2.67±0.65	4.12±0.67	<0.001	1.44 (1.08, 1.81)	0.349	0.08	0.103 (–0.073, 0.363)	0.037	
3DP vs.									
Long orifice diameter	2.43±0.46	4.12±0.67	<0.001	1.69 (1.37, 2.01)	0.756	<0.001	0.133 (–0.03, 0.453)	<0.001	
Perimeter-derived circumferential orifice diameter	2.22±0.41	4.12±0.67	<0.001	1.90 (1.59, 2.20)	0.837	<0.001	0.11 (–0.02, 0.40)	<0.001	
Perimeter-derived maximum orifice diameter	3.49±0.64	4.12±0.67	0.01	0.63 (0.26, 0.99)	0.837	<0.001	0.575 (–0.094, 0.859)	<0.001	
3DV vs.									
Long orifice diameter	2.62±0.47	4.12±0.67	<0.001	1.50 (1.17, 1.82)	0.898	<0.001	0.194 (–0.021, 0.568)	<0.001	
Perimeter-derived circumferential orifice diameter	2.37±0.39	4.12±0.67	<0.001	1.75 (1.44, 2.05)	0.956	<0.001	0.138 (–0.015, 0.469)	<0.001	
Perimeter-derived maximum orifice diameter	3.72±0.62	4.12±0.67	0.031	0.40 (0.04, 0.76)	0.956	<0.001	0.802 (–0.054, 0.951)	<0.001	
VATS vs.									
Long orifice diameter	3.79±0.59	4.12±0.67	0.067	0.33 (–0.02, 0.68)	0.863	<0.001	0.758 (0.180, 0.914)	<0.001	

Data are expressed as the mean ± standard deviation. 2D, two-dimensional; 3D, three-dimensional; TEE, transesophageal echocardiography; VATS, video-assisted thoracic surgery; 3DP, 3D-transesophageal echocardiography with multiplanar reformatting; 3DV, 3D-transesophageal echocardiography with volumetric measurement; CI, confidence interval; ICC, intraclass correlation coefficient.

however, the related Pearson correlation coefficients for these modalities were 0.837 ($P<0.001$), 0.956 ($P<0.001$), and 0.863 ($P<0.001$), respectively. Moreover, all these ICCs showed good agreement (0.575, 95% CI: –0.094 to 0.859, $P<0.001$; 0.802, 95% CI: –0.054 to 0.951, $P<0.001$; 0.758, 95% CI: 0.180–0.914, $P<0.001$ respectively) (Table 2).

The Bland-Altman analysis showed a strong correlation

and low variability between the perimeter-derived 3DP measurement (the maximum orifice diameter), the perimeter-derived 3DV measurement (the maximum orifice diameter), VATS, and the Atriclip effective length. The variability of the mean values was 3.85%, 0.00%, and 11.54%, respectively, for the Atriclip effective length (Figure 2).

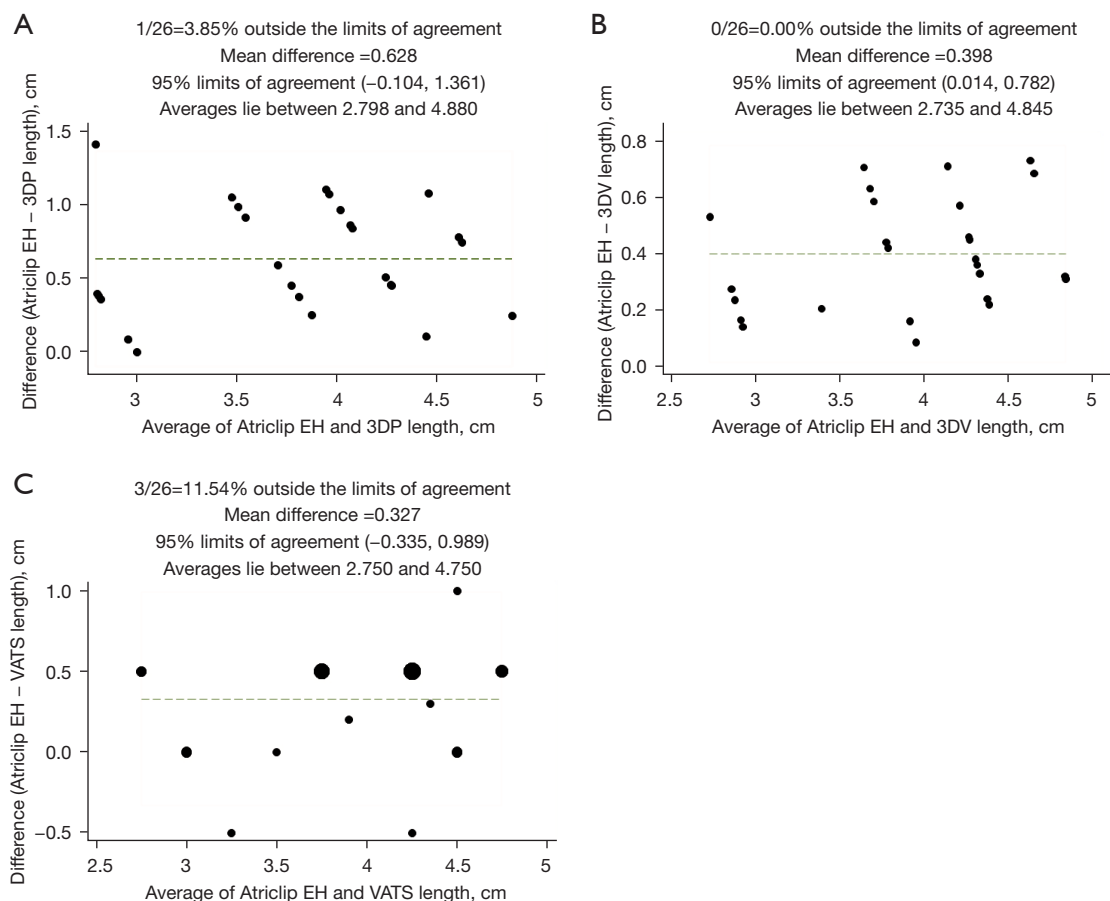


Figure 2 Bland-Altman analysis of differences in the LAA orifice diameters. (A) 3DP *vs.* Atriclip EH; (B) 3DV *vs.* Atriclip EH; (C) VATS *vs.* Atriclip EH. EH, effective length; 3DP, 3D-transesophageal echocardiography with multiplanar reformatting; 3DV, 3D-transesophageal echocardiography with volumetric measurement; VATS, video-assisted thoracic surgery; LAA, left atrial appendage.

Comparison of sizing effectiveness between 3D-TEE and VATS in LAA clipping

Using the Atriclip size as the control, the mean difference in the LAA diameter was 0.21 cm (95% CI: -0.15 to 0.57, $P=0.247$) in the perimeter-derived 3DP sizing (the maximum orifice diameter), 0.08 cm (95% CI: -0.29 to 0.44, $P=0.675$) in the perimeter-derived 3DV sizing (the maximum orifice diameter), 0.27 cm (95% CI: -0.07 to 0.60, $P=0.112$) in the VATS sizing, and -0.23 cm (95% CI: -0.57 to 0.10, $P=0.172$) in the VATS + 0.5 cm sizing; however, the related Pearson correlation coefficients for these modalities were 0.808 ($P<0.001$), 0.938 ($P<0.001$), 0.851 ($P<0.001$), and 0.851 ($P<0.001$), respectively. Moreover, all these ICCs showed good agreement (0.772, 95% CI: 0.505–0.897, $P<0.001$;

0.934, 95% CI: 0.856–0.970, $P<0.001$; 0.756, 95% CI: 0.333–0.903, $P<0.001$; 0.775, 95% CI: 0.440–0.905, $P<0.001$, respectively) (Table 3).

The Bland-Altman analysis showed a strong correlation and low variability between the perimeter-derived 3DP sizing (the maximum orifice diameter), perimeter-derived 3DV sizing (the maximum orifice diameter), VATS sizing, VATS + 0.5 cm sizing, and Atriclip size. The variability of the mean values was 3.85%, 3.85%, 11.54%, and 11.54%, respectively (Figure 3).

For the distribution of matched sizing, the perimeter-derived 3DV sizing method (20/26) had a higher proportion than the perimeter-derived 3DP sizing (11/26, $P=0.011$), VATS sizing (9/26, $P=0.002$), and VATS + 0.5 cm sizing (14/26, $P=0.08$) method (Table 4 and Figure 4).

Table 3 Comparison of sizing effectiveness between 3D-TEE, and VATS in LAA clipping

Variables	Other sizing (cm)	Atriclep sizing (cm)	P	Mean difference (95% CI)	Pearson correlation		ICC	
					R	P	R (95% CI)	P
3DP vs.								
Perimeter-derived sizing	3.90±0.63	4.12±0.67	0.247	0.21 (−0.15, 0.57)	0.808	<0.001	0.772 (0.505, 0.897)	<0.001
3DV vs.								
Perimeter-derived sizing	4.04±0.65	4.12±0.67	0.675	0.08 (−0.29, 0.44)	0.938	<0.001	0.934 (0.856, 0.970)	<0.001
VATS vs.								
Maximum orifice diameter sizing	3.84±0.52	4.12±0.67	0.112	0.27 (−0.07, 0.60)	0.851	<0.001	0.756 (0.333, 0.903)	<0.001
Maximum orifice diameter + 0.5 cm sizing	4.35±0.52	4.12±0.67	0.172	−0.23 (−0.57, 0.10)	0.851	<0.001	0.775 (0.440, 0.905)	<0.001

Data are expressed as the mean ± standard deviation. 3D, three-dimensional; TEE, transesophageal echocardiography; VATS, video-assisted thoracic surgery; LAA, left atrial appendage; 3DP, 3D-transesophageal echocardiography with multiplanar reformatting; 3DV, 3D-transesophageal echocardiography with volumetric measurement; CI, confidence interval; ICC, intraclass correlation coefficient.

Prospective comparison between 2D-TEE, 3D-TEE, and LAA excision margin length

Using the LAA excision margin length as the control, the mean difference in the LAA diameter was 1.17 cm (95% CI: 0.71–1.62, $P < 0.001$) in the maximum orifice diameter of 2D-TEE, 0.15 cm (95% CI: −0.32 to 0.61, $P = 0.523$) in the perimeter-derived 3DP measurement (the maximum orifice diameter), and 0.03 cm (95% CI: −0.47 to 0.53, $P = 0.901$) in the perimeter-derived 3DV measurement (the maximum orifice diameter), and the related Pearson correlation coefficients for these modalities were 0.760 ($P = 0.001$), 0.843 ($P < 0.001$), and 0.963 ($P < 0.001$), respectively. Both the ICCs for the perimeter-derived 3DP measurement (the maximum orifice diameter) and 3DV measurement (the maximum orifice diameter) showed good agreement (0.812, 95% CI: 0.54–0.93, $P < 0.001$; 0.963, 95% CI: 0.90–0.99, $P < 0.001$; respectively) (Table 5). Similarly, good correlations were also found in the Bland-Altman analysis, with 6.7% variability in the mean values for the LAA excision margin length.

Discussion

This study first compared the sizing effects measured by 2D, 3D-TEE, and VATS, and then established a novel sizing method with 3D-TEE for the LAA clip device. This method, especially the 3DV measurement, was superior to the direct measurement in the VATS view. Moreover, we confirmed the effective sizing role of 3D-TEE in

the selected LAA VATS excision patients with AF. More importantly, it is proposed that TEE can not only evaluate LAA thrombus, Atriclep location, and effect, but can also be used for preoperative accurate sizing (20).

The role of TEE in the sizing of LAA occluders has been studied for many years. Moreover, different LAA occluders have different sizing parameters (17,21). Both 2D-TEE (the maximum orifice diameter) and 3D-TEE (the maximum orifice diameter, area- or perimeter-derived circumferential orifice diameter) have been effectively used for occlusion sizing. In addition, 3D-TEE has been shown to be superior to 2D-TEE for various types of LAA orifice shapes. Recently, research has shown that the perimeter-derived circumferential orifice diameter had the best performance in occlusion sizing among three 3D-TEE parameters (22). Consistently, our study found that the novel 3D-TEE measurement was superior in LAA clipping via VATS compared with the 2D-TEE or VATS direct measurements. Technically, the LAA orifice might have a linetype shape after LAA clipping but a round shape after LAA occlusion. Thus, we first used the perimeter-derived maximum (perimeter/2) rather than the circumferential (perimeter/ π) orifice diameter to effectively predict the LAA clip size, as evidenced by a large mean difference between perimeter-derived circumferential orifice diameter and Atriclep effective length [3DP: 1.90 cm (95% CI: 1.59–2.20); 3DV: 1.75 cm (95% CI: 1.44–2.05)] (Table 2).

It is not yet known whether the commonly used landmarks (the LCX and the highest point of the Coumadin

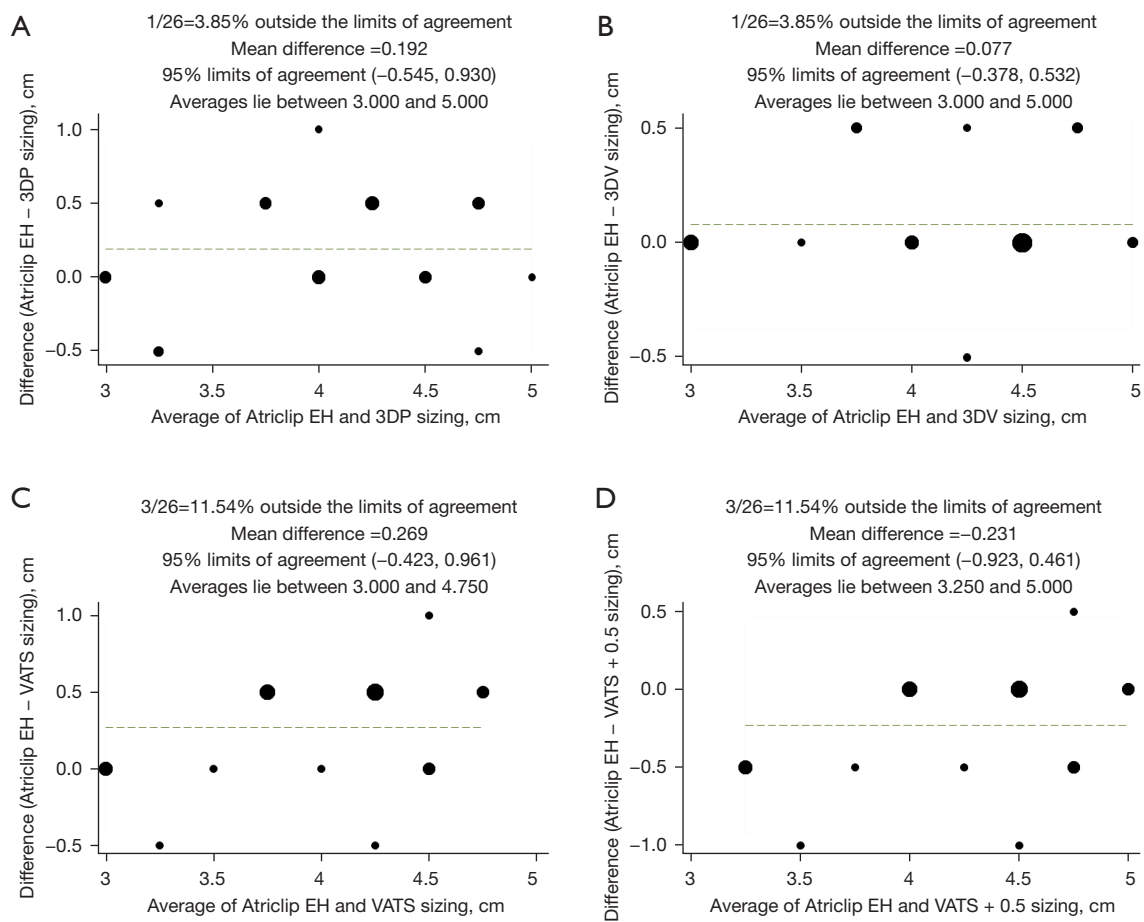


Figure 3 Bland-Altman analysis of differences in the sizing. (A) 3DP *vs.* Atriclip EH; (B) 3DV *vs.* Atriclip EH; (C) VATS *vs.* Atriclip EH; (D) VATS + 0.5 *vs.* Atriclip EH. EH, effective length; 3DP, 3D-transesophageal echocardiography with multiplanar reformatting; 3DV, 3D-transesophageal echocardiography with volumetric measurement; VATS, video-assisted thoracic surgery.

Table 4 Distribution of matched sizing in 3D-TEE and VATS

Variables	Matched sizing (n)	Unmatched sizing (n)	% of patients	P value (vs. 3DV)
3DP	11	15	42.3	0.011
3DV	20	6	76.9	–
VATS	9	17	34.6	0.002
VATS + 0.5 cm	14	12	53.8	0.08

3D, three-dimensional; TEE, transesophageal echocardiography; VATS, video-assisted thoracic surgery; 3DP, 3D-transesophageal echocardiography with multiplanar reformatting; 3DV, 3D-transesophageal echocardiography with volumetric measurement; n, number.

ridge) for TEE assessment in LAA orifice measurement during LAA occlusion are suitable for LAA clipping devices. Currently, the sizing parameters based on the landmarks among different LAA occluders are quite different (17,21). In our experience, these two procedures (the intracardiac *vs.* epicardial surgical approach) are quite different, and

the landmarks for the LAA clipping should be closer to the pericardium. To simulate the epicardial thoroscopic procedure of the LAA, we chose the LCX and LSPV orifice (the root of the Coumadin ridge) as the two reference points. Additionally, we prospectively enrolled 15 patients undergoing VATS LAA excision, and the results showed

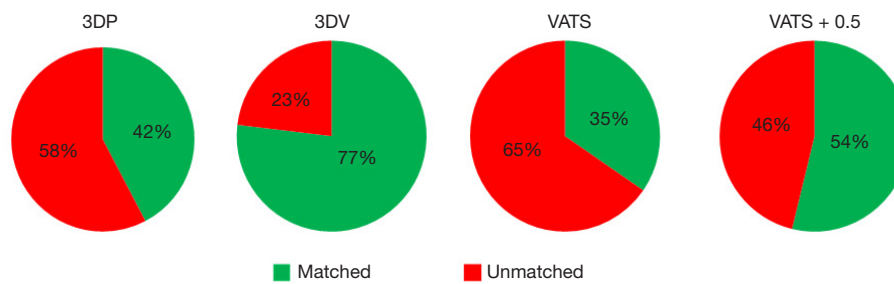


Figure 4 Distribution of matched sizing in 3D-TEE and VATS. 3DP, 3D-transesophageal echocardiography with multiplanar reformatting; 3DV, 3D-transesophageal echocardiography with volumetric measurement; VATS, video-assisted thoracic surgery.

Table 5 Comparison between 2D-TEE, 3D-TEE, and LAA excision margin length

Variables	Other measurements (cm)	LAA excision margin length (cm)	P value	Mean difference (95% CI)	Pearson correlation		ICC		
					R	P	R (95% CI)	P	
2D-TEE vs.									
Long orifice diameter	2.70±0.52	3.88±0.68	<0.001	1.17 (0.71, 1.62)	0.760	0.001	0.260 (−0.06, 0.67)	0.001	
3DP vs.									
Long orifice diameter	2.54±0.47	3.88±0.68	<0.001	1.34 (0.90, 1.77)	0.661	0.007	0.172 (−0.06, 0.55)	0.006	
Perimeter-derived maximum orifice diameter	3.72±0.56	3.88±0.68	0.523	0.15 (−0.32, 0.61)	0.843	<0.001	0.812 (0.54, 0.93)	<0.001	
3DV vs.									
Long orifice diameter	2.59±0.52	3.88±0.68	<0.001	1.29 (0.83, 1.74)	0.841	<0.001	0.253 (−0.04, 0.67)	<0.001	
Perimeter-derived maximum orifice diameter	3.84±0.64	3.88±0.68	0.901	0.03 (−0.47, 0.53)	0.963	<0.001	0.963 (0.90, 0.99)	<0.001	

Data are expressed as the mean ± standard deviation. 2D, two-dimensional; 3D, three-dimensional; TEE, transesophageal echocardiography; LAA, left atrial appendage; 3DP, 3D-transesophageal echocardiography with multiplanar reformatting; 3DV, 3D-transesophageal echocardiography with volumetric measurement; CI, confidence interval; ICC, intraclass correlation coefficient.

an excellent agreement between 3D-TEE and the excision length. Taken together, the novel landmarks for LAA clip are effective in sizing, and merit further promotion in the clinical setting.

In this study, we also compared the accuracy of the VATS direct measurement and the 3D-TEE measurement in determining LAA sizing. The effects of the VATS direct measurement and 3D-TEE measurement in the accuracy of LAA sizing. Theoretically, the surgical approach and view in VATS are very similar to those in the LAA clip delivery. In this study, we found that the VATS measurement showed better agreement than the 3DP measurement but was less accurate than the 3DV measurement. In addition, we also estimated the sizing accuracy of assumed adding 0.5 cm based on the VATS sizing; however, no obvious

improvement was observed. The precise underlying mechanisms for these differences could not be confirmed; however, one potential major explanation is that VATS is similar to the 2D-TEE long orifice diameter for the LAA *in situ*, and the error of measurement agreement could be greatly affected by the various LAA orifice shapes (23-27). However, the undue effect of different LAA shapes can be minimized in the 3D-TEE perimeter-derived maximum orifice diameter.

3D-TEE has been widely used for device sizing in LAA interventional procedures; however, the difference in the sizing accuracy of the 3DP and 3DV measurements has not yet been investigated. Previous studies have shown that the novel 3DP technique, which has improved accuracy, still uses a 2D plane acquired from the 3D data set for

the structures, while the 3DV measurement enables the comprehensive identification of the complex asymmetric 3D borderline and non-planarity of the structures (28,29). In addition, the 3DV measurement measures the anatomic structure independently to patient hemodynamic variability (29). In this study, we found that the 3DV measurement was more accurate in sizing the LAA clip device than the 3DP measurement. Additionally, the results involving 15 prospective patients undergoing VATS LAA excision also confirmed the advantage of the 3DV technique.

Our study had several limitations. First, multidetector computed tomography measurements were not used for the LAA (30). Thus, its role in sizing remains unknown. Second, unlike other occluder sizing studies, we did not evaluate the role of the area-derived circumferential orifice diameter in sizing the LAA device (14,17). The LAA orifice shape is linetype after clipping, but circular after occluder introduction. The difference in the final closure of the LAA orifice is very likely to enlarge the transformation deviation. Third, the sample size of our study was relatively small. Fourth, we cannot rule out the effect of the potential volume status on LAA clip sizing during imaging acquisition (31-33). Finally, no TEE assessment was conducted during the follow-up period after patient discharge.

Conclusions

Our study showed that 3D-TEE might be used in the sizing of the novel LAA clip device via the VATS approach in patients with AF. The 3DV measurement was superior to the VATS measurement. These findings might also apply to LAA VATS excision patients with AF.

Acknowledgments

Funding: This study was supported by a grant from the Ministry of Science and Technology of People's Republic of China (No. 2016YFC1302001). The funder had no role in the study design, data collection, data analysis, data interpretation, or writing of the manuscript.

Footnote

Reporting Checklist: The authors have completed the STROBE reporting checklist. Available at <https://qims.amegroups.com/article/view/10.21037/qims-23-900/rc>

Conflicts of Interest: All authors have completed the ICMJE uniform disclosure form (available at <https://qims.amegroups.com/article/view/10.21037/qims-23-900/coif>). The authors have no conflicts of interest to declare.

Ethical Statement: The authors are accountable for all aspects of the work in ensuring that questions related to the accuracy or integrity of any part of the work are appropriately investigated and resolved. This study was conducted in accordance with the Declaration of Helsinki (as revised in 2013). The study was approved by the Independent Ethics Committee of Fuwai Hospital, and all patients provided written informed consent.

Open Access Statement: This is an Open Access article distributed in accordance with the Creative Commons Attribution-NonCommercial-NoDerivs 4.0 International License (CC BY-NC-ND 4.0), which permits the non-commercial replication and distribution of the article with the strict proviso that no changes or edits are made and the original work is properly cited (including links to both the formal publication through the relevant DOI and the license). See: <https://creativecommons.org/licenses/by-nc-nd/4.0/>.

References

1. Pathak R, Lau DH, Mahajan R, Sanders P. Structural and Functional Remodeling of the Left Atrium: Clinical and Therapeutic Implications for Atrial Fibrillation. *J Atr Fibrillation* 2013;6:986.
2. Kannel WB, Wolf PA, Benjamin EJ, Levy D. Prevalence, incidence, prognosis, and predisposing conditions for atrial fibrillation: population-based estimates. *Am J Cardiol* 1998;82:2N-9N.
3. Knecht S, Wilton SB, Haïssaguerre M. The 2010 update of the ESC guidelines for the management of atrial fibrillation. *Circ J* 2010;74:2534-7.
4. Furie KL, Goldstein LB, Albers GW, Khatri P, Neyens R, Turakhia MP, Turan TN, Wood KA, American Heart Association Stroke Council; Council on Quality of Care and Outcomes Research, Council on Cardiovascular Nursing; Council on Clinical Cardiology, Council on Peripheral Vascular Disease. Oral antithrombotic agents for the prevention of stroke in nonvalvular atrial fibrillation: a science advisory for healthcare professionals from the American Heart Association/American Stroke Association. *Stroke* 2012;43:3442-53. Erratum in: *Stroke*

- 2012;43:e181. Erratum in: *Stroke* 2013;44:e20.
5. Beigel R, Wunderlich NC, Ho SY, Arsanjani R, Siegel RJ. The left atrial appendage: anatomy, function, and noninvasive evaluation. *JACC Cardiovasc Imaging* 2014;7:1251-65.
 6. Stoddard MF, Dawkins PR, Prince CR, Ammash NM. Left atrial appendage thrombus is not uncommon in patients with acute atrial fibrillation and a recent embolic event: a transesophageal echocardiographic study. *J Am Coll Cardiol* 1995;25:452-9.
 7. Ailawadi G, Gerdisch MW, Harvey RL, Hooker RL, Damiano RJ Jr, Salamon T, Mack MJ. Exclusion of the left atrial appendage with a novel device: early results of a multicenter trial. *J Thorac Cardiovasc Surg* 2011;142:1002-9, 1009.e1.
 8. Mokracek A, Kurfirsh V, Bulava A, Hanis J, Tesarik R, Pesl L. Thoracoscopic Occlusion of the Left Atrial Appendage. *Innovations (Phila)* 2015;10:179-82.
 9. Zheng Y, Rao CF, Chen SP, He L, Hou JF, Zheng Z. Surgical left atrial appendage occlusion in patients with atrial fibrillation undergoing mechanical heart valve replacement. *Chin Med J (Engl)* 2020;133:1891-9.
 10. Li H, Qu J, Yu Y, Zhang H, Rao C, Liu S, Zheng L, Lu B, Zheng Z. Sinoatrial nodal artery injury in thoracoscopic epicardial ablation for atrial fibrillation. *Eur J Cardiothorac Surg* 2020. [Epub ahead of print]. doi: 10.1093/ejcts/ezaa317.
 11. Zheng Z, Li H, Liu S, Gao G, Yu C, Lin H, Meng Y. Box lesion or bi-atrial lesion set for atrial fibrillation during thoracoscopic epicardial ablation. *Interact Cardiovasc Thorac Surg* 2022;34:1-8.
 12. Zheng Z, Yao Y, Li H, Zheng L, Liu S, Lin H, Duan F. Simultaneous hybrid maze procedure for long-standing persistent atrial fibrillation with dilated atrium. *JTCVS Tech* 2021;5:34-42.
 13. Wunderlich NC, Beigel R, Swaans MJ, Ho SY, Siegel RJ. Percutaneous interventions for left atrial appendage exclusion: options, assessment, and imaging using 2D and 3D echocardiography. *JACC Cardiovasc Imaging* 2015;8:472-88.
 14. Schmidt-Salzman M, Meincke F, Kreidel F, Spangenberg T, Ghanem A, Kuck KH, Bergmann MW. Improved Algorithm for Ostium Size Assessment in Watchman Left Atrial Appendage Occlusion Using Three-Dimensional Echocardiography. *J Invasive Cardiol* 2017;29:232-8.
 15. Vainrib AF, Harb SC, Jaber W, Benenstein RJ, Aizer A, Chinitz LA, Saric M. Left Atrial Appendage Occlusion/Exclusion: Procedural Image Guidance with Transesophageal Echocardiography. *J Am Soc Echocardiogr* 2018;31:454-74.
 16. Wang DD, Forbes TJ, Lee JC, Eng MH. Echocardiographic Imaging for Left Atrial Appendage Occlusion: Transesophageal Echocardiography and Intracardiac Echocardiographic Imaging. *Interv Cardiol Clin* 2018;7:219-28.
 17. Zhang L, Cong T, Liu A. Percutaneous closure of the left atrial appendage: The value of real time 3D transesophageal echocardiography and the intraoperative change in the size of the left atrial appendage. *Echocardiography* 2019;36:537-45.
 18. Gilhofer TS, Saw J. Periprocedural Imaging for Left Atrial Appendage Closure: Computed Tomography, Transesophageal Echocardiography, and Intracardiac Echocardiography. *Card Electrophysiol Clin* 2020;12:55-65.
 19. Koo TK, Li MY. A Guideline of Selecting and Reporting Intraclass Correlation Coefficients for Reliability Research. *J Chiropr Med* 2016;15:155-63.
 20. Rosati F, de Maat GE, Valente MAE, Mariani MA, Benussi S. Surgical clip closure of the left atrial appendage. *J Cardiovasc Electrophysiol* 2021;32:2865-72.
 21. Tan NY, Yasin OZ, Sugrue A, El Sabbagh A, Foley TA, Asirvatham SJ. Anatomy and Physiologic Roles of the Left Atrial Appendage: Implications for Endocardial and Epicardial Device Closure. *Interv Cardiol Clin* 2018;7:185-99.
 22. Yosefy C, Azhibekov Y, Brodtkin B, Khalameizer V, Katz A, Laish-Farkash A. Rotational method simplifies 3-dimensional measurement of left atrial appendage dimensions during transesophageal echocardiography. *Cardiovasc Ultrasound* 2016;14:36.
 23. Jahanyar J, Mastrobuoni S, Munoz DE, Aphram G, de Kerchove L, El Khoury G. Aortic annulus elevation for aortic valve and root replacement. *J Card Surg* 2022;37:1101-3.
 24. Pinto Teixeira P, Ramos R, Rio P, Moura Branco L, Portugal G, Abreu A, Galrinho A, Marques H, Figueiredo L, Cruz Ferreira R. Modified continuity equation using left ventricular outflow tract three-dimensional imaging for aortic valve area estimation. *Echocardiography* 2017;34:978-85.
 25. Kumar V, Sengottuvelu G, Singh VP, Rastogi V, Seth A. Transcatheter Aortic Valve Implantation for Severe Bicuspid Aortic Stenosis - 2 Years Follow up Experience From India. *Front Cardiovasc Med* 2022;9:817705.
 26. Khalique OK, Hamid NB, White JM, Bae DJ, Kodali SK,

- Nazif TM, Vahl TP, Paradis JM, George I, Leon MB, Hahn RT. Impact of Methodologic Differences in Three-Dimensional Echocardiographic Measurements of the Aortic Annulus Compared with Computed Tomographic Angiography Before Transcatheter Aortic Valve Replacement. *J Am Soc Echocardiogr* 2017;30:414-21.
27. Prihadi EA, van Rosendaal PJ, Vollema EM, Bax JJ, Delgado V, Ajmone Marsan N. Feasibility, Accuracy, and Reproducibility of Aortic Annular and Root Sizing for Transcatheter Aortic Valve Replacement Using Novel Automated Three-Dimensional Echocardiographic Software: Comparison with Multi-Detector Row Computed Tomography. *J Am Soc Echocardiogr* 2018;31:505-514.e3.
 28. Karamnov S, Burbano-Vera N, Huang CC, Fox JA, Shernan SK. Echocardiographic Assessment of Mitral Stenosis Orifice Area: A Comparison of a Novel Three-Dimensional Method Versus Conventional Techniques. *Anesth Analg* 2017;125:774-80.
 29. Karamnov S, Burbano-Vera N, Shook DC, Fox JA, Shernan SK. A Novel 3-Dimensional Approach for the Echocardiographic Evaluation of Mitral Valve Area After Repair for Degenerative Disease. *Anesth Analg* 2020;130:300-6.
 30. Xu B, Betancor J, Sato K, Harb S, Abdur Rehman K, Patel K, Kumar A, Cremer PC, Jaber W, Rodriguez LL, Schoenhagen P, Wazni O. Computed tomography measurement of the left atrial appendage for optimal sizing of the Watchman device. *J Cardiovasc Comput Tomogr* 2018;12:50-5.
 31. Spencer RJ, DeJong P, Fahmy P, Lempereur M, Tsang MYC, Gin KG, Lee PK, Nair P, Tsang TSM, Jue J, Saw J. Changes in Left Atrial Appendage Dimensions Following Volume Loading During Percutaneous Left Atrial Appendage Closure. *JACC Cardiovasc Interv* 2015;8:1935-41.
 32. Al-Kassou B, Tzikas A, Stock F, Neikes F, Völz A, Omran H. A comparison of two-dimensional and real-time 3D transoesophageal echocardiography and angiography for assessing the left atrial appendage anatomy for sizing a left atrial appendage occlusion system: impact of volume loading. *EuroIntervention* 2017;12:2083-91.
 33. Freitas-Ferraz AB, Bernier M, O'Connor K, Beaudoin J, Champagne J, Paradis JM, O'Hara G, Muntané-Carol G, Alperi A, Faroux L, Junquera L, Rodés-Cabau J. Safety and effects of volume loading during transesophageal echocardiography in the pre-procedural work-up for left atrial appendage closure. *Cardiovasc Ultrasound* 2021;19:3.

Cite this article as: Duan F, Li H, Zhou C, Li H, Tao J, Kang W, Yu M, Zheng Z. Novel sizing role of 3D transesophageal echocardiography in a novel left atrial appendage clip device for patients undergoing video-assisted atrial fibrillation ablation: a cohort study. *Quant Imaging Med Surg* 2024;14(2):1335-1347. doi: 10.21037/qims-23-900